AIR SPARGING REMEDIATION: A STUDY ON HETEROGENEITY AND AIR MOBILITY REDUCTION

[1]S.S. Di Julio and [2]A.S. Drucker

[1]California State University, Northridge, Northridge, CA 91330; [1]Phone: (805) 667-2496, [1]Fax: (805) 667-7062, [1]E-mail: sdijulio@ecs.csun.edu; [2]NFESC, US Navy; [2]Phone: (805) 982-4847, [2]E-mail: adrucke@nfesc.navy.mil.

ABSTRACT

Contaminated groundwater is a widespread problem often requiring innovative technology to remediate. The purpose of this paper is to present the laboratory results of air sparging models. Initial tests used very fine porous media (glass beads-packed column) to represent a relatively homogeneous soil samples. Subsequent testing employed budded core samples taken from a site of interest to represent more realistic, heterogeneous samples. 1,1,1 Trichloroethane (TCA) was used as the dissolved contaminant to represent BTEX/ gasoline contamination; however, results obtained here can be applied to any NAPL-dissolved phase. A technique based on foam injection is proposed and is demonstrated to reduce air mobility. This reduction in air mobility has potential to improve contaminant removal. Laboratory results are compared with predictions of a numerical model, which is an advection-diffusion air sparge simulation model. Sensitivity analysis of the numerical model provides the range of some key parameters used to screen/evaluate air sparging as the remediation method for a given contaminated site of interest. Eventual scaleup of the model to an actual site application can be justified by the favorable results presented in this paper.

Key words: *remediation, air sparging, NAPL, foam*

BACKGROUND

The efficiency of air sparging as a groundwater remediation process depends to a large extent on the contact time and contact area of air with contaminated water. A number of investigators have conducted laboratory or field studies, or numerical simulation, in order to better understand air distribution and a few have conducted studies to measure the removal rate of contaminants from groundwater. A majority of these studies chose mostly homogeneous porous media, either 2D/3D glass-beads or sand packs, or core samples for laboratory studies, and/or homogeneous strata for field studies. Ji et al. (1993), Ahfeld et al. (1994), and Clayton (1998) have demonstrated the tendency of air channels developing in response to heterogeneity at both pore and larger scale in coarse to fine homogeneous sand. The transition from pore-scale viscous fingering to macroscopic capillary air channeling is estimated by Clayton (1998) to occur at air-entry pressure of about 15 to 20 cm of water. Since this is a low air-entry pressure, it is very likely that air channeling occurs, as was seen in all 18 laboratory experiments carried out by Clayton (1998).

It is important to realize that the mechanism of contaminant removal, in such by-passed regions both in homogeneous and heterogeneous porous media, is severely diffusion limited (Clayton, 1998; Ji and Ahfled, 1993; Clayton and Nelson, 1995; Clark, 1996; Choa, 1998; Brusseau, 1991). Plummer et al. (1997) observed channeling in their 2-D homogeneous, medium-grained glass beads model and the homogeneous sand pack of comparable permeability, density, and porosity representing both horizontal and vertical well configurations. The air distribution was more uniform for the horizontal well, suggesting that more of the porous media is impacted by air flow. We have also observed (discussed in Results Section) that in our core studies the contaminant recovery is more efficient in the horizontally cut cores than the vertically cut, indicating the adverse effect of soil stratification on contaminant recovery rate.

McKay and Acomb (1996) and Schima et al. (1996) used neutron moisture probe and cross-bore hole resistivity, respectively, to measure percentage of fluid displaced and air distribution during air sparging at two wells in a homogeneous formation consisting of uniform sands. They observed an initial rapid lateral expansion followed by consolidation of the region. They also observed inconsistent readings in less permeable, heterogeneous formations, indicating the inconsistent behavior of air flow in such formations.

Chao et al. (1998) have developed water-to-air mass transfer for a number of VOCs during air sparging in soil columns packed with coarse, medium, or fine sand or glass bead. They used a reaction numerical model and assumed concentration in the bulk phase remains constant due to slow diffusion of VOC in the aqueous phase to the air-water interface as compared to rapid volatilization of VOCs at the air-water interface. Therefore, they have modeled the interface mass transfer alone. Their results indicated that, depending on the VOC sparged, the estimated fraction of total volume affected by air sparging varied from 5 to 20% for fine sand, but may be as high as 50% for coarse sand, where more channels are expected to form. This observation has been made by others (Ji et al. 1993, and Clayton 1998), as well as us; our sensitivity runs, discussed later in this paper, indicate that contaminant *recovery near the interface* increases as the air channel density and VOC diffusivity increase. However, as our results indicate, the *overall contaminant recovery efficiency decreases when air channels or bypassing occurs*. This is mainly due to overall decrease in air saturation, and as seen in our laboratory results, the contaminant recovery time will increase drastically. Hence it is best to reduce or eliminate channeling as proposed by foam injection, discussed later in this paper. We also share the observation made by Chao et al. (1998) that there seem to be an optimum mass transfer flow rate.

Ahlfed et al. (1994) have conceptually described the air sparging process and they note that in heterogeneous, stratified formations in which sparging is often applied, the pattern of air movement through the subsurface is complex. This complexity is largely driven by variation in grain size, capillary resistance, and intrinsic permeability of the porous media. In addition, operating parameters such as airflow rate, injection pressure, and depth and cross-sectional area of injection will also affect the contaminant recovery process. As far as the authors know, no laboratory study has specifically involved heterogeneous core studies. Hence we hope that our laboratory results on comparison between contaminant recoveries in relatively homogeneous and heterogeneous porous media, and the proposed foam injection, instead of air injection, will aid in improving the contaminant recovery for an air sparging process. The proposed process may also decrease the remediation or cleanup time, which is of important concern during field operation.

EXPERIMENTAL AND NUMERICAL MODELS

a. Experimental Setup and Procedure

To study contaminant recovery in a relatively homogeneous porous media, a glass-bead packed column, constructed of clear acrylic pipe, packed with beads of an average grain diameter of 67 microns, was used. Both ends of the column were sealed with recessed end caps around the injection and production ports to prevent leakage. To allow a dispersed flow of air through the column, a 40-micron sintered-bronze filter, 0.32 cm in diameter and length, was positioned on the centerline at the bottom of the glass bead-packed column. This filter represented the slotted portion of a sparge well, distributing air along its length. Positioned at the top of the column was a 11.4 cm long acrylic pipe, which was sealed with another end cap. This void space was created to allow the water to swell (rise due to displaced volume by air). A positive pressure transducer and a differential pressure transducer were used to measure inlet pressure and pressure drop across the column. The water vapor in the air was removed prior to injection and its flow rate was controlled and measured accurately by a digital flow system. The effluent air was sampled by a gas chromatograph. At the end of each run, it was extremely important to remove residual contaminant. This was done by flushing the column with warm water and hot air for a number of days.

To study contaminant recovery in heterogeneous porous media, a composite core model was used. The core samples taken from the site of interest were composed of silty sand, sandy siltstone, silty sandstone, and fine to coarse-grained sandstone. The composite core assembly consisted of three core samples, cut either vertically or horizontally. A sleeve of heat-shrinkable Teflon™ tubing was slid over the composite cores with screens and end plates at the two ends to hold the sand grains in place; the composite cores were then housed in a Hassler pressure cell. Mineral oil was used for application of overburden pressure. Properties of all three laboratory models are given in Table 1.

Table 1. Porous Media Properties

Porous Media Properties	Glass Bead Pack	Vertical Composite Core	Horizontal Composite Core
Length (cm)	61	14.14	15.06
Diameter (cm)	5.72	2.54	2.54
Permeability, k (md)	0.39	15.2	52.1
Porosity, ϕ (%)	36.3	24	35.5
Pore volume, ml	448	26.1	23.5

Benzene, toluene, ethyl benzene, and xylene are all constituents of BTEX, the largest regulated component of gasoline contamination. In an effort to reduce the number of variables in the laboratory study, focus was primarily given to the remediation of benzene, the most stringently regulated contaminant. However, due to the health hazard associated with exposure to benzene, 1,1,1 trichloroethane (TCA) was selected as a suitable alternative to benzene, having similar solubility, vapor pressure, and Henry's constant (ratio of vapor pressure to solubility). Other properties such as molecular weight, density, boiling point, melting point, and specific heat were also considered for comparison. Table 2 gives a comparison of the chemical properties of benzene with cyclohexane, toluene, and 1,1,1 trichloroethane; chemicals used as suitable alternatives. Because the contaminant is in dissolved phase only, its specific gravity does not play an important role and the experimental results can be applied to both LNAPL and DNAPL remediation.

Both the glass-bead pack and the composite cores were saturated with a solution of water and TCA at three different concentrations of 10, 25, and 50 ppm. Low-pressure air of 1.41 - 1.68 atm (6-10 psig) was injected through the bottom of the saturated glass bead-packed column or the composite-core assembly. Contaminant removal rate at three different flow rates of 15, 20, and 30 ml/min were studied. Air then flowed to the top where it was sampled intermittently, at intervals of 3 - 14 minutes, by a gas chromatograph to measure the concentration of TCA in the effluent, as shown in Figure 1.

b. Numerical Model Description

Analytical and numerical models provide insight into the air sparging mass transfer process. Rabideau and Blayden (1998) have

Table 2. Chemical Properties of Various Contaminants

Chemical Properties	Benzene	Cyclohexane	Toluene	Trichloroethane
Solubility (g/l)	1.77	58	0.53	4.4
Vapor pressure (kPa)	12.7	13.1	3.8	16.5
Molecular weight (g/mol)	78.11	84.16	92.14	133.4
Melting point (°C)	5.5	6.5	-95	-30
Boiling point (°C)	80.1	81	111	74
Density (g/ml)	0.8765	0.7785	0.8669	1.3303
Specific heat (J/g-K @ 25 °C)	1.74	1.84	1.71	1.08
Henry's Constant (Bar-m/mol @ 25 °C)	5.6×10^{-3}	1.9×10^{-1}	6.6×10^{-3}	4.3×10^{-3}

Data from CRC Handbook of Chemistry and Physics, CRC Press, 73 Edition 1992-1993

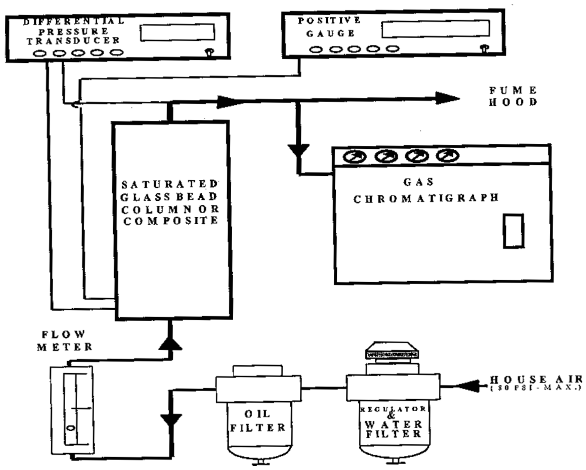

Figure 1. Schematic of Experimental Setup

reviewed the literature on modeling work done on air sparging and have categorized the numerical models into two types:

1. Mechanistic models, or multi-dimensional, PDE, known also as compositional multidimensional models for fluid flow and contaminant removal studies. These numerical models are commonly used in the oil industry due to availability of extensive site characterization. Such data are usually not cost-effective for remediation sites where operation costs are minimized and comprehensive site characterizations are not available.

2. Reactor models, on the other hand, are simpler and can handle mass removal, volume of fluid circulating through the source zone, and air channel development.

A number of investigators have used multiphase flow simulation to model air sparging. But as Clayton (1998) points out, multiphase flow simulations are unable to handle air channeling without special considerations to represent flow in individual stream tubes, which are not interconnected.

A reactor model based upon past visual studies, which simulated flow dynamics of air sparging (Ji et al., 1993) and Wilson’s (1992) proposed general n-compartment model, was developed. Between the advective air channel regions of the soil column, VOC liquid phase transport, as simulated by the model, was assumed to be diffusion limited. To facilitate data analysis, the model was written using Visual Basic Application (VBA). The numerical model had the capability to simulate the cycling on and off of the sparge system, a practice some agree has the potential to reduce costs and increase remediation efficiency (Hinchee, 1994; Acomb and McKay, 1996). In addition, the model can be used to help predict the extent of post-remedial contaminant rebound by simulating groundwater contaminants as they diffuse towards equilibrium concentrations. About 60% of the 32 case studies evaluated showed poor performance (not sufficient for site closure) due to substantial rebound following an initial contaminant concentration reduction (Bass, 1996). Generally a period of 6-12 months is required for rebound to fully develop. In some cases this rebound may be related to rise in water table, and hence desorption of contaminant. Our results showed that the slow diffusion of contaminant towards air channels may also be responsible for rebound of dissolved contaminant concentration.

Because the water velocity is negligible (McCray and Falta, 1977), the aqueous-phase dispersion is neglected. The contaminant vaporizes at the interface, and its distribution within the air channel is assumed to be instantaneous

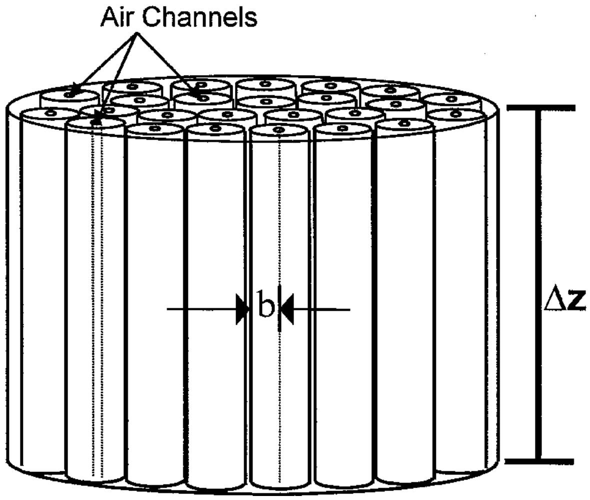

Figure 2. Annular Aqueous and Air Channel Regions of Model

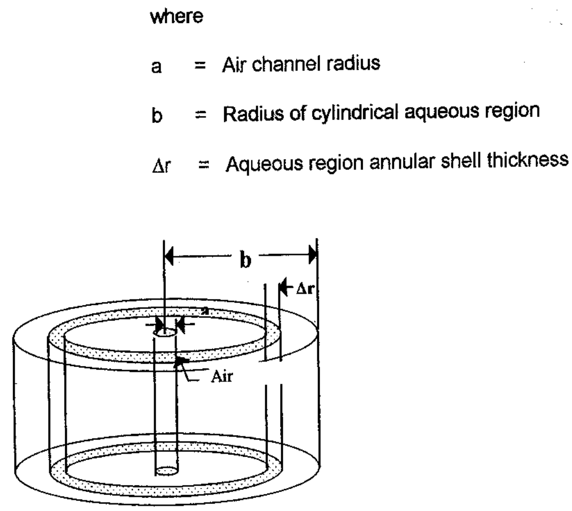

Figure 3. Annular Shells Within a Single Aqueous Region

and thus is considered an equilibrium process, described by Henry's Law (Equation 1), which is the best-case assumption. Our measurements also indicated that equilibrium is not reached in the early part of contaminant recovery curves, when advection forces are predominant.

$$C^g = K_h C^l \tag{1}$$

where:

C^g = Molar concentrations of compund in gas phase - (g moles/m^3)

C^l = Molar concentration of compound in liquid phase - (g moles/m^3)

K_h = Henry's law constant - dimensionless

Based on work performed by Wilson et. al. (1992) and Roberts et. al. (1993), the soil column was modeled as a composite of evenly spaced cylindrical air channels with a surrounding nonadvective aqueous region (a radius of "b") illustrated in Figure 2. All air channel and cylindrical aqueous regions are to be equal in length and circumference. The soil column of height, "h", is to be divided into equal vertical-length (Δz) sections as shown in Figure 2. Figure 3 illustrates how each cylindrical aqueous region in each soil column element is divided into equal-thickness (Δr) annular shells. Additionally, a tortuosity parameter (Lpath or path length coefficient) was used to make the parallel air channels resemble the tree-like air channels observed by investigators.

Combining Fick's first law relationship of binary diffusion with Henry's Law, along with equations to describe the geometry, results in the following equation, which represents the diffusion transport of the contaminant through the aqueous region:

$$\frac{dC^W}{dt} = \frac{M}{Vol} = \frac{2\pi\Delta z D}{\phi\Delta r\Delta V_j}\left[-r_{j+1}\left(C^W{}_{j+1}\right)+r_j\left(C^w_{j-1}-C^w_j\right)\right]$$

where:

$\phi =$ Soil porosity - (L^3/ L^3)

Vol = Volume - (L^3)

$C^w =$ Concentration of the contaminant in the solvent (water) - (m/ L^3)

The following equation represents the contaminant transport once it has entered the air channel:

$$\frac{dC^w}{dt} = \frac{-4D\left(C_i^g / K_h - C^w n\right)}{\phi a \Delta r} + \frac{V_c\left(C^g{}_{i+1} - C^g{}_i\right)}{\phi \pi a^2 \Delta z(Channel\,\#)}$$

For details of the numerical model, please refer to Drucker (1995,1996).

c. Foam Injection to Reduce Air Mobility

The capacitance or dead-end pore model was originally proposed to explain the concentration "tail" observed in breakthrough curves of displacements. This tail is more pronounced in carbonate than in sand stones because the pore structure of a typical carbonate is more heterogeneous (Raimondi and Torcaso, 1964; Stalkup, 1970; Shelton and Schneider, 1975; Spence and Watkins, 1980). Similarly we have observed the more pronounced tailing phenomenon here when the results of contaminant recovery for glass beads are compared with that of the core, even though the contaminant exists as a dissolved phase only. This leads one to believe that in our study, air channeling or by-passing in heterogeneous cores resulted in the inefficiency in contaminant recovery, leading into longer recovery times than the relatively homogeneous glass bead packs. This is also supported by the results of sensitivity analysis on "a" (air channel radius) as seen in the Results section.

This problem may be remedied by using foaming surfactants, which tend to encapsulate air and form foam. The reduction of air mobility increases air residence time and the contact area between air and the contaminated water, which can result in improved contaminant recovery. Foams are dispersion of gas bubbles in liquids. Such dispersions are normally quite unstable, unless surfactant is added to the liquid, which greatly improves the stability. Previous foam studies in reservoir engineering have demonstrated the tendency of foams to preferentially plugging channels or higher permeable regions in porous media. Additionally air mobility is reduced via an increase in air viscosity and decrease in air-relative permeability (a reduction as high as 200-600 fold), while gas saturation remains unchanged (Khan, 1965; Bernard and Holm, 1964). This is attributed to blocking of pore throats due to gas films. In a parallel core flood study, Di Julio (1989) demonstrated the ability of foam to reduce CO_2 gas mobility by plugging air channels in higher permeable core and to diverting CO_2 to lower permeability core. The foam injection resulted in an incremental oil recovery of 33.6%. It is expected that foam injection in the air sparge process reduces air mobility and hence provides a significant reduction in contaminant recovery time.

RESULTS

a. Model Sensitivity Analysis

A sensitivity analysis was performed by varying several input parameters and observing their impact on normalized residual mass of contaminant. The input variables used to conduct the analysis were "a" (air channel radius), "D" (diffusivity constant), "Kh" (Henry's constant), and "Vc" (air injection flow rate). Results of this analysis are presented in Figures 4 - 7.

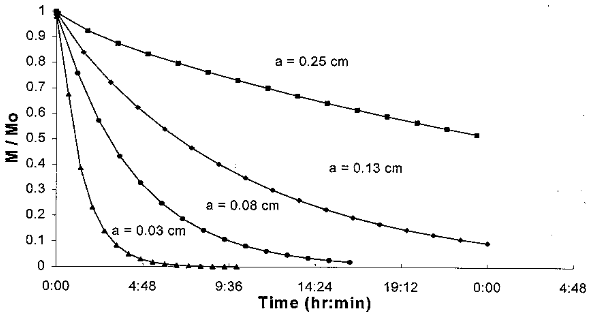

Figure 4. Normalized Residual Mass vs. Remediation Time (“a” is varied)

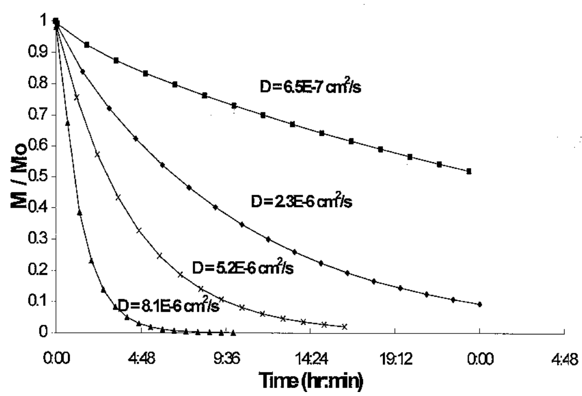

Figure 5. Normalized Residual Mass vs. Remediation Time (“D” is varied)

Normalized values of residual mass, M/Mo, for a given range of “a”, are shown in Figure 4. As the value of the air channel radius, a, is changed, it proportionally affects the value of “b,” the radius of the aqueous region surrounding the air channel. For instance, if the value “a” is decreased, the value of “b” is also decreased (due to an increase in air channel number density), causing the remediation rate to improve. Therefore, to improve contaminant removal efficiency, it is desirable to promote a relatively large number of air channels, having small radii, within a given volume of saturated soil. In the limit, this may be represented by evenly distributed air saturation within a given zone.

The diffusivity constant, D, has no direct bearing on the channel geometry but has a significant effect on the contaminant removal rate. Most VOC diffusion coefficients will fall in the range between 2.54E-7 to 3.0E-6 cm^2/s. The contaminant removal rates in the form of M/Mo are illustrated in Figure 5. From the figure it is evident that the increase in value of diffusivity improves the contaminant removal rate. This result is expected due to the model being diffusion limited.

Henry’s constant, Kh, has a pronounced but limited effect on air sparging remediation efficiency, as shown in Figure 6. In this particular case, Henry’s constant has an upper limit of approximately 0.35 (i.e., Kh values larger than 0.35 will not improve upon the remediation rate). The lower boundary of Kh values, such as Kh = 0.01, illustrates how a relatively low volatilization rate limits the contaminant removal rate. Therefore, an analysis such as this can be useful in determining the effectiveness of air sparging on the removal rate of contaminants with lower values of Kh, such as semi-volatile organic solvents.

The volumetric flow rate of injected air has a direct bearing on the air saturation within saturated soil. It is expected that an increase of airflow rate will increase the air saturation and hence increase the number and diameter of the air channels. However, to investigate only the effect of air volumetric flow rate on rate of contaminant removal, air saturation is held constant, while the flow rate is raised or lowered, as shown in Figure 7. The lower limit of air-flow, Vc = 0.016 cm^3/s, in Figure 7, is an example of flow rate becoming too small to

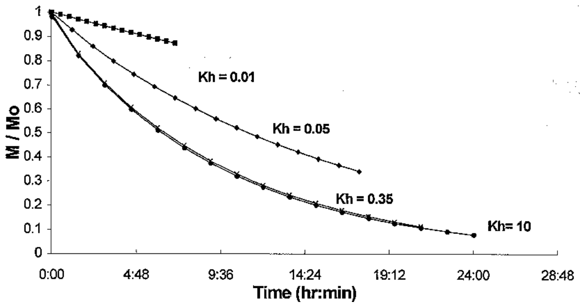

Figure 6. Normalized Residual Mass vs. Remediation Time ("K_h" is varied)

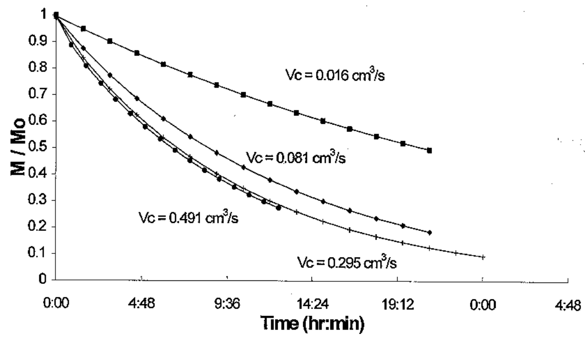

Figure 7. Normalized Residual Mass vs. Remediation Time ("Vc" is varied)

efficiently remove the contaminant volatilized in the air channel. Lower limits of airflow such as this are encountered at the perimeter of a sparge well's region of influence. The upper limit of effectiveness of raising the airflow rate is realized at or slightly less than Vc = 0.295 cm^3/s. Therefore, air injection greater than 0.295 cm^3/s will only serve to increase the cleanup costs associated with sparging the contaminated groundwater. This is an important observation, since the air sparging process is a diffusion-limited process. An increase in air-injection flow rate will not have a significant effect on the rate of contaminant diffusion and removal, but may only improve the vaporization (according to Henry's Law) and hence its subsequent advection by air.

b. Laboratory Results

The removal rate is believed to be controlled by two distinct processes of advection and diffusion. Initially the rate of contaminant removal is controlled by advection. Contaminant is removed by relatively quick vaporization from the air channel wall and subsequent advection by air, until the contaminant concentration in the air channel reduces below that in the aqueous phase, at which time the diffusion process will begin to dominate the removal rate. These two regions of flow regimes: advection-controlled and diffusion-controlled, are seen as the initial peaks followed by an asymptotic behavior in all of our contaminant removal curves, respectively.

Contaminant recovery in glass bead packs were measured at three different air-injection flow rates (10, 20, and 30 ml/min) for three different initial concentrations of (10, 25, and 50 ppm TCA in water). Figure 8 shows the contaminant recoveries at three different flow rates for initial concentration of 25 ppm. Figure 9 shows a similar curve for 50 ppm initial concentration. The increase in air-injection flow rate increases the contaminant recovery slightly. Comparing the contaminant recovery for 50 ppm and 25 ppm at air-flow rate of 20 ml/min, the higher peak for 50 ppm, indicates higher convective recovery very early on. However, this higher recovery is not sustained during the second portion of the curve, which is diffusion-limited, shown as the asymptotic recovery, leading to lower overall percentage recovery.

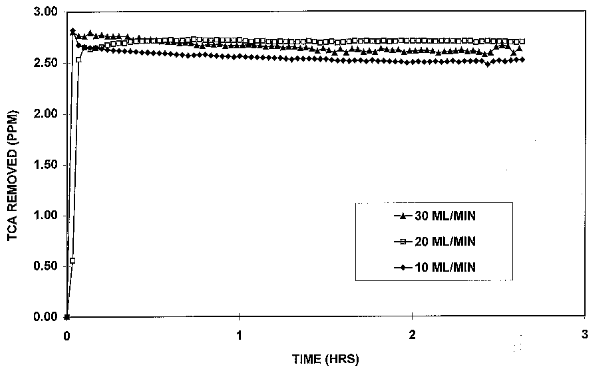

Figure 8. Cont. Recovery for Initial TCA Concent. of 25 ppm—Glass Bead Pack

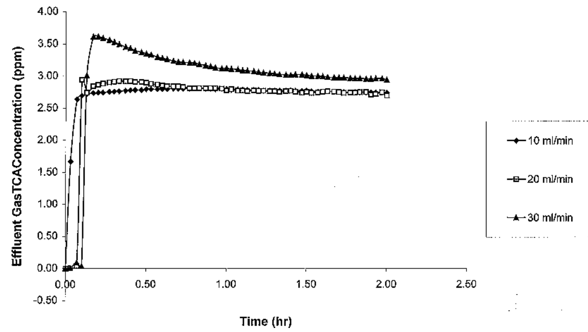

Figure 9. Cont. Recovery for Initial TCA Concent. of 50 ppm—Glass Bead Pack

To study the effect of heterogeneity on contaminant recovery, measurements on glass bead pack may be compared with those from the cores and also measurements on horizontally cut cores may be compared with those for the vertically cut cores, which are more heterogeneous and stratified.

Figures 10 and 11 show results of three air sparging runs for the horizontal and vertical composite cores, respectively. Concentrations of the contaminant, TCA, in effluent air, as a function of time for air injection rates of 15, 20, and 30 ml/min are compared. Note that these results are for initial concentration of 25 ppm TCA in water, used to saturate the core prior to air injection. Results for the horizontal composite core look more like the glass bead pack run; the contaminant removal curves are flatter at generally higher concentrations of contaminant and with less tailing effect, as compared with those for the vertical composite core. This behavior could be attributed to the higher heterogeneity of the vertical composite core, where more channeling/bypassing takes place and hence the removal efficiency is inconsistent and lower. As the initial concentration of contaminant is increased, the optimum flow rate, for which contaminant recovery is maximum, also increases. For example, we observed that the optimum flow rate for 10 ppm was 10 ml/min, while that of 25 ppm was about 20 ml/min. We obtained reasonably good reproducibility of the recovery profile and the percent of total contaminant removed. But we had difficulty with cleaning the cores after each run.

Our experimental results on glass bead packs show less channeling than our core studies, as seen in the shape of contaminant recovery profile and the shorter recovery time (about 4 hr recovery time for the glass bead pack versus 24 hr recovery time for the composite core, estimated based on cumulative recoveries), considering that the glass bead pack has a pore volume which is about 22.4 times that of the composite cores. This can also be observed when experimental results are compared with the numerical model predictions, which assume the contaminant recovery takes place via air channels; the predicted profile matches the core studies better due to its inherent heterogeneity and hence predominant recovery via air channels.

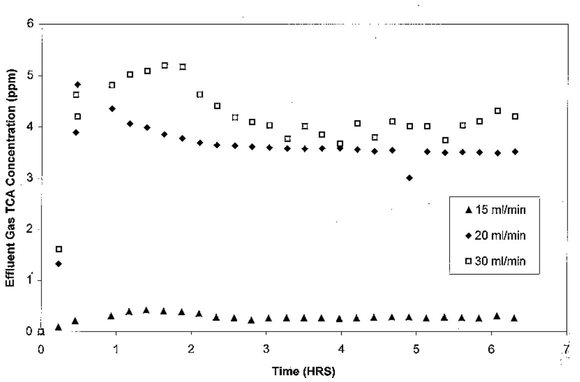

Figure 10. Cont. Recovery for Initial TCA Concent. of 25 ppm—Horizontal Composite Core

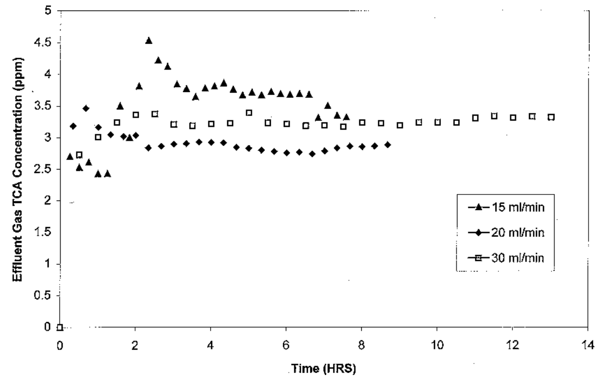

Figure 11. Cont. Recovery for Initial TCA Concent. of 25 ppm—Vertical Composite Core

Results of two experiments on glass bead and composite cores are compared with the numerical model prediction as shown in Figures 12 and 13. Figure 12 for the glass bead pack is at 10 ppm and 15 ml/min, while Figure 13 is for vertical composite core at 50 ppm and 15 ml/min initial TCA concentration and air-injection flow rate, respectively. The predicted concentrations are matched against the experimental values by varying the parameter *a*, *air channel radius*, which in effect also changes the density of air channels. Table 3 shows the input and calculated variables used for simulation. The peak values of contaminant concentration are approximately 1/4 to 1/10 of the estimated equilibrium values, based on Henry's Law, which assumes instantaneous distribution of contaminant within the air channels. As expected, Henry's law provides the upper limit of contaminant concentration in the effluent air. The laboratory measurement results in Figure 13 show a leveling off at 3.5 ppm, after 3 1/3 hours, while the model prediction tends to asymptotically approach zero-contaminant concentration. This discrepancy may be attributed to dispersion and/or adsorption processes which were not included in our numerical model. Even with this discrepancy, one may still acquire a conservative prediction of the air sparge remediation rate, if one were to scale up the numerical model to simulate air sparging at the field scale. The existing model has considerable potential for evolving into an accurate field-scale model. Once developed, the field-scale numerical model could be used in the design of a full-size air sparge system by determining air sparge well spacing and placement, air injection rate, injection pressure, and rate of remediation.

Since the numerical model allows for the contaminant removal through air channels only, the better match between measurements in the core samples and predictions indicates the existence of channels in heterogeneous samples, and hence the need for reduction of air channeling. One such remedy may be foam injection.

c. Result of Foam injection

In the case considered here, the average bubble size is larger than the pore diameter and thus foam flows as a progression of films that

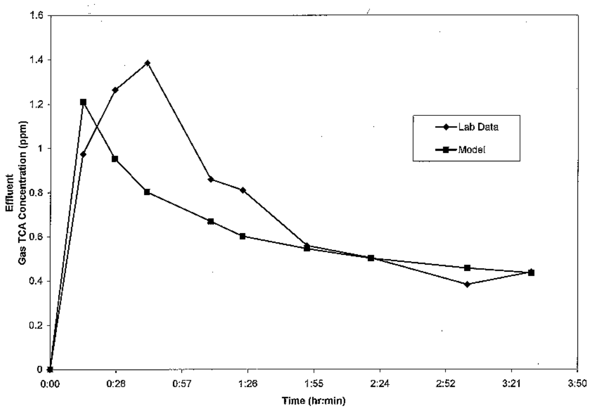

Figure 12. Comparison of Laboratory and Numeric Model Results—Glass Bead Pack

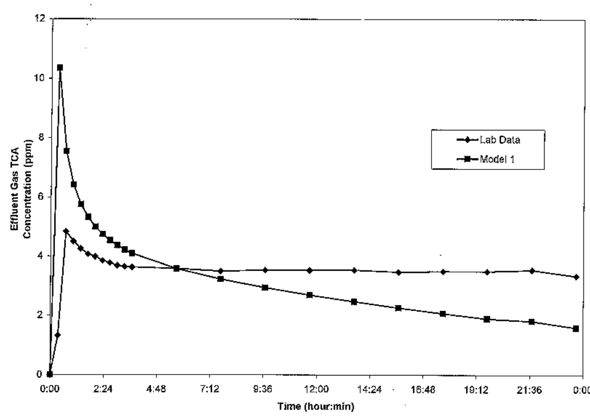

Figure 13. Comparison of Laboratory and Numeric Model Results—Composite Core

separate individual gas bubbles. Some of the undesirable features of surfactant, such as sensitivity to highly saline brine, temperature, contaminant type, and retention, need to be considered when surfactants are selected for a given site.

We used the surfactant Steol CA-460, manufactured by Stepan Company in Northfield, Ill. Steol CA-460 is an alcohol-ethoxy sulfate consisting of 15% denatured ethyl alcohol and 2% ammonium sulfate. To study the reduction of air mobility in the air sparging process, the glass bead-pack column was saturated with water and the pressure drop across the column was measured as air was injected into the column at a given flow rate. This provided the baseline pressure-drop profile. The column was then saturated with a solution of 1%-by-weight surfactant in water and again the pressure drop across the column was measured as air was injected. Note that we expected some air channeling or bypassing in the glass bead pack, which would be less than that in the composite cores. Figure 14 shows an example of the measured increase in pressure drop when air is injected into the column where surfactant is present. We observed the formation of foam within the column and the increase in pressure drop by a factor of 20 to 40 on the average, at flow rates of 53 and 20 ml/min, respectively. This drastic increase in pressure drop is attributed to decrease in air relative permeability, which results from reduction of air channels. As seen in previous studies ,the reduction of gas mobility can improve its saturation distribution and hence increase both the contact area and contact time between the air and the contaminant, resulting in an improved recovery of the contaminant from porous media.

CONCLUSION

Laboratory results from glass bead packed column and composite cores have demonstrated the effectiveness of air sparging as a remediation process. Two distinct regimes of advective-controlled and diffusion-controlled flows are observed. Measurements on composite cores showed more channeling than the relatively homogeneous glass bead packs, and hence required a much longer time for air injection and subsequent contaminant removal.

A numerical reaction model was used to conduct a sensitivity analysis by varying input parameters such as air channel radius (a), diffusion constant (D), Henry's Law constant (Kh), and injection flow rate (Vc). Results of the analysis illustrate the significance of each parameter with respect to air sparging feasibility and remediation rate. Model predictions of contaminant removal agreed fairly well with the laboratory measurement results and indicated the prominent existence of channels in heterogeneous samples, and hence the need for reduction of air channeling. Use of foaming surfactants is suggested as a method to reduce air mobility in channels. This can lead into reduction of air channeling and may improve contami-

Table 3. Input and Calculated variables for Simulation

Glass Bead Input Variables			
variable	**value**	**units**	**description**
rad	1.000	in.	radius of influence
h	24.0000	in.	sparge pt. - water table depth
Vc	0.01520	cuin/s	control panel volumetric flow rate
Kh	0.713	n/a	Henry's constant
Cjo	50.00	ppb	initial contaminant concentration
v	0.36	cuin/cuin	total soil porosity
w	0.33	cuin/cuin	water-filled soil porosity
D	1.50E-07	sqin./s	diffusion constant
Csat	1,100,000.00	ppb	contaminant saturation concentration
a	7.00E-02	in.	air channel radius
Lpath	1.4	in/in	path-length coefficient (1≤ Lpath ≤ 2)
dt	4.20	s	time interval

Glass Bead Calculated Variables				
variable	**calculation**	**value**	**units**	**description**
dz	h/cell row #	2.400	in	cell height
b	rad/(Chanl#Lpath)^.5	0.404	in	nonadvective channel radius
dr	(b-a)/9	0.037	in	nonadvective shell thickness
a factor	a/dr	1.882	in/in	air channel radius/shell thickness
channel#	(v-w) x (rad/a) ^2/Lpath	4373	n/a	airchannel number per element
ppbfactor	.001 if using ppb's	0.001	n/a	ppb calculation factor
z	dz x j	n/a	in	cell height

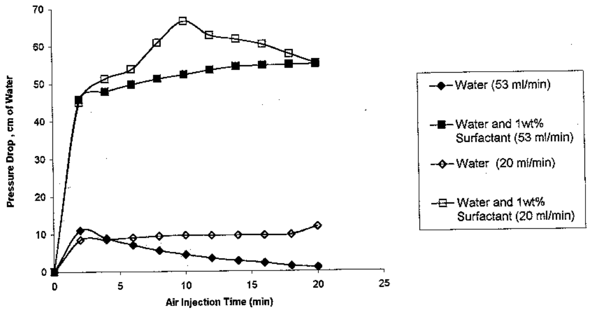

Figure 14. Foam-Induced Nobility Control Indicated by Increase in Pressure Drop

nant recovery by diverting foam to less permeable zones.

ACKNOWLEDGMENTS

We wish to thank Southern California Gas Co. for providing project funding, the California State University-Northridge engineering students who helped construct the laboratory apparatus and conduct the applicable tests, and Bill Shallenberger for guidance and review of the analysis and laboratory results.

Andrew S. Drucker (adrucke@nfesc.navy.mil) is currently an engineer at the Naval Facilities Engineering Service Center, Point Huneme, Calif. He completed the numerical analysis presented here as his master's thesis at the aforementioned university. Shoeleh Di Julio (the correspondent author, sdijulio@ecs.csun.edu) is a professor at California State University-Northridge, Mechanical Engineering Department, Northridge, CA 91330-8348.

REFERENCES

Ahlfed, D.P., A. Dahmani, and W. Ji, 1994. A conceptual model of field behavior of air sparging and its implication for application. Ground Water Monitoring and Remediation, 14, no. 4: 132-139.

Bass, D.H., and R. A. Brown, 1996. Air sparging case study database update. Proceedings of the First International Symposium on *In Situ* Air Sparging for Site Remediation. October 24 and 25, Las Vegas, Nevada.

Brusseau, M.L., 1991. Transport of organic chemicals by gas advection in structured or heterogeneous porous media: development of a model and application to column experiments. *Water Resour. Res*., Dec., 27, 12, 3189-3199.

Bernard, G.G., and L.W. Holm, 1964. Effect of foam on permeability of porous media to gas. SPE 986, presented at the Fall technical Conference and Exhibition of the Society of petroleum Engineers, Houston, Texas.

Chao, K.P., S.K. Ong, and A. Protopapas, 1998. Water-to-air mass transfer of VOCs: Laboratory-scale air sparging system. *J. of Environmental Engineering*, 124, no. 11, pp1054-1060.

Clayton, W.S., 1998. A field and laboratory investigation of air fingering during air sparging. *Ground Water Monitoring and Remediation*, 18, no. 3,134-145.

Di Julio, S. S., and A.S. Emanuel, 1989. Laboratory study of foaming surfactant for CO_2 mobility control. 1989. *SPE Reservoir Engineering*, May, 136-142

Drucker, A.S., 1995. Aliso Canyon site *in situ* remediation. M.S. Thesis. California State University, Northridge.

Drucker, A.S., and S.S. Di Julio, 1996. Groundwater cleanup, *in situ* air sparging: development of a model and application to saturated soil column experiments. Water Environment Federation, WEFTECH'96, 69th Annual Conference & Exposition, Dallas, Texas, October 5-9, 1996.

Hinchee, R.E., 1994. Air sparging for site remediation. CRC Press Inc., Boca Raton.

Ji, W., A. Dahmani, D.P. Ahlfeld, J.D. Lin, and E. Hill,1993. Laboratory study of air sparging: air flow visualization. *Ground Water Monitoring & Remediation 13, no.4:* 115-126.

Johnson, R.L., P.C. Johnson, D.B. McWhorter, R.E. Hinchee, and I. Goodman, 1993. An overview of *in situ* air sparging. *Ground Water Monit. Rev.,* Fall, 127-135.

Kearl, P.M., and N.E. Korte, 1991. Vapor extraction experiments with laboratory soil columns—implications for field programs. *Waste Management*, 121, 231-239.

Khan, S. A., 1965. The flow of foam through porous media. M.S. thesis, Stanford University.

McCray, J.E., and R.W. Falta, 1997. Numerical simulation of air sparging for remediation of NAPL contamination. *Ground Water* 35, no. 1: 99-110.

McKay, D. J., and L. J. Acomb, 1996. Neutron moisture probe measurements of fluid displacement during *in situ* air sparging. *Ground Water Monitoring and Remediation* 16, no.4: 86-94.

Plummer, C. R., J. D. Nelson, and G. S. Zumwalt. 1997. Horizontal and vertical well comparison for *in situ* air sparging. *Ground Water Monitoring and Remediation* 17, no. 1: 91-96.

Rabideau, A.J., and J.M. Blayden, 1998. Analytical model for contaminant mass removal by air sparging. *Ground Water Monitoring and Remediation*, Fall 1998, pp120-130.

Raimondi, P., and M. A. Torcaso, 1964. Distribution of oil phase obtained upon imbibition of water. *Transaction of the American institute of Mining and Mmetallurgical Engineering*, 231: 49-55.

Roberts L.A., and D.J. Wilson, 1993. Groundwater cleanup by *in situ* sparging I. modeling of dense, non-aqueous-phase liquid droplet removal. *Separation Science And Technology*, 28, 5, 1127-1143.

Schima, S., D.J. Labrecque, and P.D. Lundegrad, 1996. Monitoring air sparging using resistivity tomography. *Ground Water Monitoring and Remediation* 16, no.2: 131-138.

Stalkup, Fred I., 1970. Displacement of oil by solvent at high water saturation. *Society of Petroleum Engineers Journal*, 10:337-348.

Shelton, J.L., and F.N. Schneider, 1975. The effect of water injection on miscible flooding methods using hydrocarbons and carbon dioxide. *Society of Petroleum Engineers Journal*, 15: 217-226.

Spence, A.P. Jr., and R.W. Watkins, 1980. The effect of microscopic core hetrogeneity on miscible flood residual oil saturation. SPE 9229, presented at the 55th Annual Fall Technical Conference and Exhibition of the Society of Petroleum Engineers, Dallas, Texas.

Wilson, D.J., S. Kayano, R.D. Mutch, and A.N. Clarke, 1992. Groundwater cleanup by *in situ* sparging, I, mathematical modeling. *Separation Science and Technology*, 27 no. 8 & 9: 1023-1041.